the case of a simple diatomic molecule such as CO, then, the nature of the STM image may be affected by the adsorbate orientation and electronic bonding properties in a fashion that is yet to be understood. As exemplified here, however, the information on binding site occupancies supplied by IRAS constitutes the critical element not only in corroborating the STM data, but enabling the real-space structures to be matched to definite CO coordination geometries. In this regard, then, the vibrational spectra fulfills the same role in conjunction with STM as is the case with LEED structural data.

It is interesting to note that a related (2 × 2) structure to that for the present Rh(111) system, with $\theta_{CO} = 0.75$, has also been observed by using STM for CO on Pt(111) in 0.1 M $HClO_4$.[3] However, the images on Pt(111) differ somewhat from those for the present (2 × 2) structure on Rh(111), the former by themselves being suggestive of adsorption on a single type of site.[3a] Further detailed studies combining STM and IRAS on this and other surfaces should yield substantial insight into the factors controlling, as well as the nature of, such adlayer structures.

**Acknowledgment.** Some experimental assistance was provided by Xudong Jiang. We are grateful to Dr. M. Van Hove for helpful advice regarding his LEED structures. S.C.C. acknowledges a fellowship from the W.R. Grace Foundation. This work is supported by grants from the National Science Foundation and the Office of Naval Research (to M.J.W.), and additionally by the Industrial Associates Program at Purdue University funded in part by Dow Chemical Co. and BP America (to B.C.S.).

# Periodicities in the Correlation of Nuclear Magnetic Deshielding and Compression of Interstitial Atoms in Metal Clusters

**Joan Mason**

*Contribution from the Department of Chemistry, The Open University, Milton Keynes MK7 6AA, U.K.* *Received January 10, 1991*

**Abstract:** The correlation of NMR shift with compression in a cluster cavity, previously demonstrated for interstitial carbides and nitrides, is extended to borides. Interstitial borides and oxides (so far measured) also follow the carbide–nitride pattern of increase in shielding of the interstitial (relative to benchmark shifts such as those of hydrides and organic compounds) across the row of the periodic table, as contraction of the normal covalent radius relieves the compression. Similarly, the shielding of butterfly interstitials increases as compression is relieved by decrease in the $M_WIM_W$ angle. These patterns can be rationalized to some extent in terms of the factors determining the local paramagnetic circulation; large increases in shielding on protonation of a butterfly interstitial show the deshielding contribution of weakly bonding (quasi-lone-pair) electrons in low-lying LUMOs. However, the magnitudes of the diamagnetic and paramagnetic contributions (calculated as Ramsey shielding terms) from the cluster metals bonded to the interstitial are such that they must contribute to the shielding patterns, notably to shielding changes with increase in nuclearity (with irregular changes in cavity size) and to the increase in shielding of the interstitial down the group of the metal (as the cavity size increases).

## Introduction

The chemical shift in NMR spectroscopy is (by definition) sensitive to local geometry, and there are many correlations with bond or angle strain.[1] High shielding is observed in small rings: cyclopropane holds the high-shielding record for $^{13}C$ in hydrocarbons, the shielding decreasing with increase in ring size,[2] and similar relationships are observed for nitrogen shifts in c-$(CH_2)_nNH$ compounds.[3] Phosphorus is highly shielded in phosphirane c-$C_2H_4PH$ ($\delta(^{31}P)$-341),[4] and the $P_4$ molecule holds the high-shielding record in phosphorus NMR spectroscopy ($\delta(^{31}P$-461).[5] Anomalous *de*shieldings, however, are observed in four-membered rings.[6] A well-known "steric" correlation in organic chemistry is the increase in carbon shielding with a $\gamma$-substituent in contrast to deshielding by $\alpha$-, $\beta$-, and $\delta$-substituents.[7]

In coordination chemistry, the dependence of phosphorus shielding on the size of chelate rings has diagnostic value: in (diphenylphosphine)alkane chelates the $^{31}P$ shielding is high for dppm, low for dppe, and normal for dppp (i.e. similar to that for $M-PPh_2R$).[8] *De*shielding is found when there are distortions due to the presence of bulky ligands: thus the phosphorus shifts of 54 tertiary phosphines in *trans*-$[PdCl_2L_2]$ complexes increase with the Tolman cone angle (*o*-tolyl- and 1-naphthylphosphines excepted).[9] The shielding of an element E in an ER group (R = alkyl) decreases more steeply in the sequence of increasing bulk, Me > Et > $Pr^i$ > $Bu^t$, than in the inductive sequence Me > Et > $Pr^n$ > $Bu^n$.

We have now shown for carbides and nitrides that nuclear magnetic deshielding $\delta(I)$ of an interstitial nucleus increases with compression of the interstitial atom (I) in a metal cluster (the interstitial radius $r(I)$ being defined as $r(I) = (r(MI)_{av} - r(MM)_{av})/2$, where M is a metal bonded to the interstitial atom) and that the deshielding decreases from carbides to nitrides (for analogous clusters), as decrease in the covalent radius of the interstitial relieves the compression.[10] This correlation can now be extended to include recent measurements of interstitial borides and oxides. The compression itself is not, of course, an explanation of the deshielding, which must be found in the factors determining the paramagnetic and diamagnetic circulations,[11,12] but the pe-

(1) Mason, J., Ed. *Multinuclear NMR*; Plenum: New York, 1987.
(2) Stothers, J. B. *Carbon-13 NMR Spectroscopy*; Academic Press: New York, 1972; p 60.
(3) Crimaldi, K.; Lichter, R. L. *J. Org. Chem.* **1980**, *45*, 1277. Duthaler, R. O.; Roberts, J. D. *J. Magn. Reson.* **1979**, *34*, 129.
(4) Wagner, R. I.; Freeman, L. D.; Goldwhite, H.; Rowsell, D. G. *J. Am. Chem. Soc.* **1967**, *89*, 1102.
(5) Crutchfield, M. M.; Dungan, C. H.; Van Wazer, J. R. *Top. Phosphorus Chem.* **1967**, *5*, 239.
(6) Lambert, J. B.; Wharry, S. M.; Block, E.; Bazzi, A. A. *J. Org. Chem.* **1983**, *48*, 3982.
(7) Grant, D. M.; Paul, E. G. *J. Am. Chem. Soc.* **1964**, *86*, 2984.
(8) Hietkamp, S.; Stufkens, D. J.; Vrieze, K. *J. Organomet. Chem.* **1979**, *179*, 107. Garrou, P. E. *Chem. Rev.* **1981**, *81*, 229.
(9) Bartik, T.; Himmler, T. *J. Organomet. Chem.* **1985**, *293*, 343.
(10) Mason, J. *J. Am. Chem. Soc.* **1991**, *113*, 24.
(11) Mason, J. *Adv. Inorg. Chem. Radiochem.* **1979**, *22*, 199; **1976**, *18*, 197 and references therein.
(12) Jameson, C. J.; Mason, J. In ref 1, Chapter 3.

0002-7863/91/1513-6056$02.50/0 

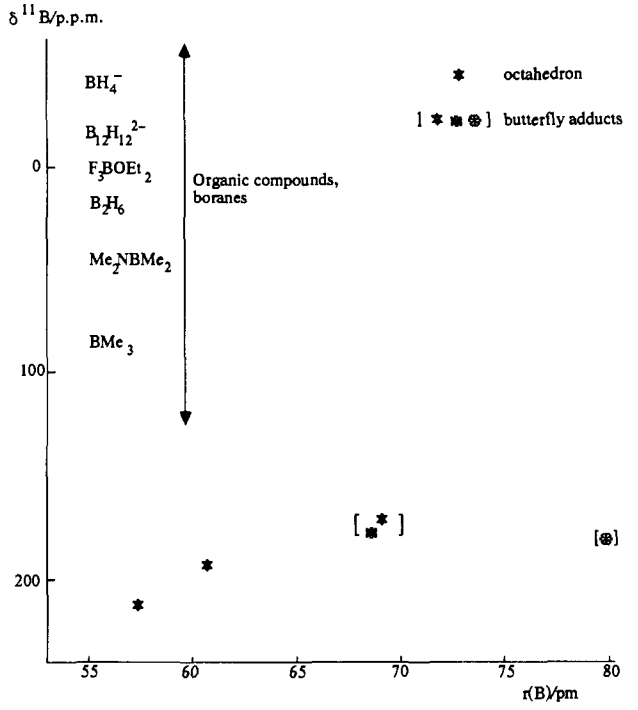


**Figure 1.** Correlation of interstitial boride shifts with atomic radius in metal clusters and with some borane and organoboron shifts.

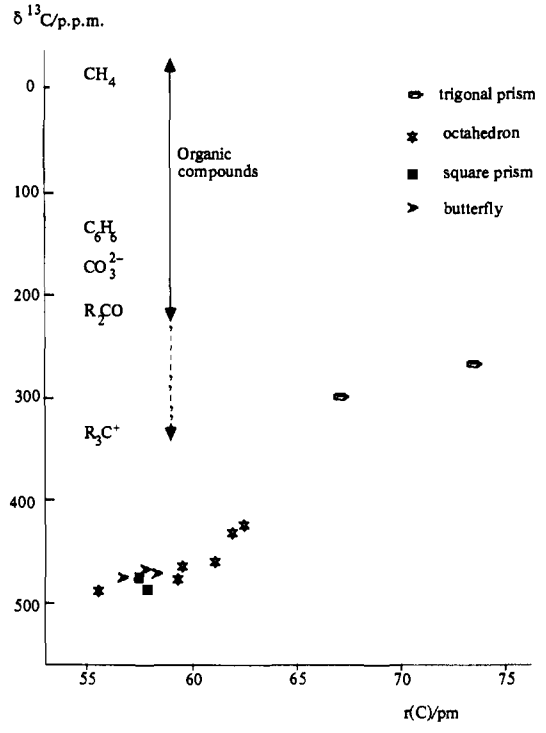


**Figure 2.** Correlation of interstitial carbide shifts with atomic radius in metal clusters and with some typical carbon shifts.

riodicity of the correlation provides evidence as to factors that are significant.

## Results and Discussion

Figures 1 and 4 and Tables I and II summarize the data on the borides and oxides, and Figures 2 and 3 are updated versions of those given for carbides and nitrides,[10] with further information on these in Tables III and IV.

Figures 1–4 need some explanation as they are constructed to give a direct comparison of shielding patterns for the different elements. Nuclear magnetic deshielding[11,12] ($\sigma$) is the algebraic sum of a diamagnetic (ground state) term ($\sigma_d$) and a paramagnetic

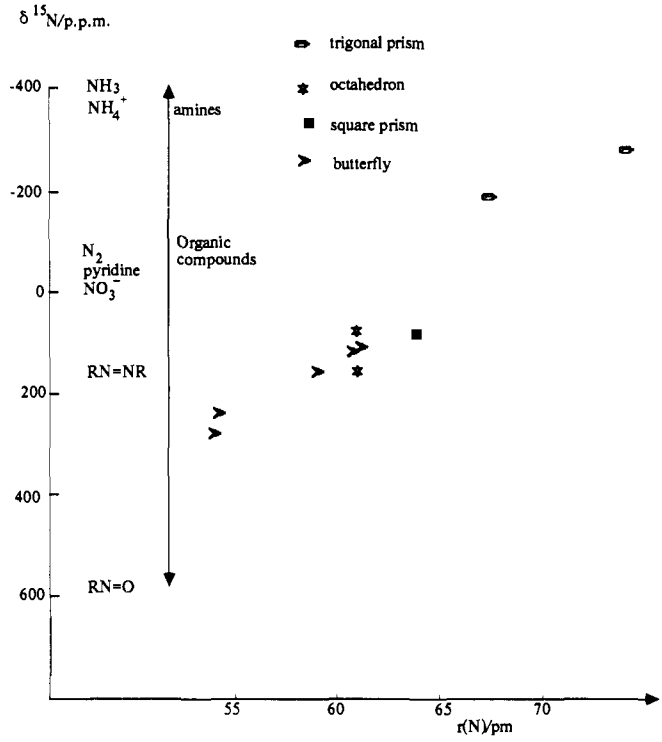


**Figure 3.** Correlation of interstitial nitride shifts with atomic radius in metal clusters and with some typical nitrogen shifts.

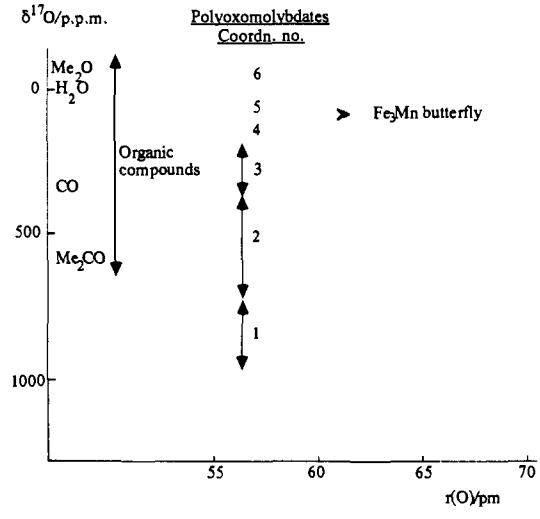


**Figure 4.** Comparison graph for interstitial oxide.

term ($\sigma_p$) arising from electronic circulations in (magnetically allowed) excited states that are mixed into the ground state by the magnetic field. $\sigma_p$ normally dominates the chemical shift for elements other than hydrogen. In approximate form, for a second-row element

$$-\sigma_p = (\mu_0/4\pi)(e^2/m^2)[\langle 0|L^2|0\rangle\langle r^{-3}\rangle_{2p}(\Delta E)^{-1}]$$

The local paramagnetic circulation is greater the closer to the nucleus (i.e. the larger the radial factor $\langle r^{-3}\rangle_{2p}$, where $r$ is the valence-p-electron radius), the smaller the excitation energy or energies ($\Delta E$), and the larger the angular momentum factor $\langle 0|L^2|0\rangle$ which generates the circulation, arising from imbalance of charge in the valence shell.[11,12] So as to be comparable for the different elements, the shifts in Figures 1–4 are scaled in proportion to the radial factors. Spectroscopic values of $\langle a_0^3 r^{-3}\rangle_{2p}$ for the free atoms are as follows: B, 0.608; C, 1.23; N, 2.46 (interpolated); O, 4.30.[13] So the scale of chemical shifts in Figure 1 is twice that of Figure 2, and correspondingly for Figures 3 and 4.

(13) Barnes, R. G.; Smith, W. V. *Phys. Rev.* **1954**, *93*, 95.

**Table I.** Boron Shifts and Atomic Radii for Interstitial Boride in Metal Clusters and Comparison Shifts for Some Protonated Borides

| cluster | $\delta(^{11}B)$/ppm | core geometry[a] | r(B)[b]/pm | ref |
|---|---|---|---|---|
| $[HRu_4(\mu_4\text{-}BH_2)(CO)_{12}]$ | 109.9 | RuHRu, 2 BHRu | | *c* |
| $[HFe_4(\mu_4\text{-}BH_2)(CO)_{12}]$ | 116 | FeHFe, 2 BHFe | | *d, e* |
| $[HRu_4(\mu_4\text{-}BH)(CO)_{12}]^-$ | 142.2 | RuHRu, BHRu | | *c* |
| $[HFe_4(\mu_4\text{-}BH)(CO)_{12}]^-$ | 150.0 | FeHFe, BHFe | | *f* |
| $[Fe_4(\mu_4\text{-}BH)(CO)_{12}]^{2-}$ | 153.0 | BHFe | | *e* |
| $[HRu_4(\mu_6\text{-}B)(CO)_{12}(AuPPh_3)_2]$ | 170.0 | $Ru_4$ bu, RuHRu, Au–Au bond ($C_2$)<br>$AuPPh_3$ bridges $BRu_w$ | 69.1 | *c* |
| $[HFe_4(\mu_6\text{-}B)(CO)_{12}(Au_2dppe)]$ | 179 | FeHFe, ns | | *g* |
| $[HFe_4(\mu_6\text{-}B)(CO)_{12}(AuPEt_3)_2]$ | 179 | FeHFe, Au–Au bond ($C_2$)<br>each $AuPEt_3$ bridges $BFe_w$ edge | 68.9 | *h* |
| $[Fe_4(\mu_7\text{-}B)(CO)_{12}(AuPPh_3)_3]^-$ | 183 | $Au^1$ caps $Fe_h{}^1Fe_w{}^4$–B face<br>$Au^2$ bridges $Fe_w{}^3$–B edge<br>$Au^3$ caps $Fe_w{}^4$–$BAu^2$ face<br>$Au^1$–$Au^2$ bond | [75] | *i* |
| $[Fe_4(\mu_6\text{-}B)(CO)_{12}(AuPPh_3)_2]^-$ | 192.2 | ns | | *j* |
| $[HRu_6(\mu_6\text{-}B)(CO)_{17}]$ | 193.8 | oct, RuHRu | 60.6 | *k* |
| $[Ru_6(\mu_6\text{-}B)(CO)_{17}]^-$ | 196 | oct, ns | | *k* |
| $[Fe_4Rh_2(\mu_6\text{-}B)(CO)_{16}]^-$ | 205 | oct, cis, ns | | *l* |
| | 211 | oct, trans | 57.5 | *l* |

[a] bu = butterfly; ns = no structure determination; oct = octahedron. $C_2$ is a symmetry label. Subscripts h and w differentiate hinge and wing metals. [b] For comparability, the boron radius in the $AuPR_3$ adducts of ($M_4$) butterfly clusters refer only to the $M_4B$ unit. [c] Chipperfield, A. K.; Housecroft, C. E.; Rheingold, A. L. *Organometallics* **1990**, *9*, 681. [d] Wong, K. S.; Scheidt, W. R.; Fehlner, T. P. *J. Am. Chem. Soc.* **1982**, *104*, 1111. [e] Rath, N. P.; Fehlner, T. P. *J. Am. Chem. Soc.* **1987**, *109*, 5273. [f] Housecroft, C. E.; Buhl, M. L.; Long, G. J.; Fehlner, T. P. *J. Am. Chem. Soc.* **1987**, *109*, 3323. [g] Housecroft, C. E. Oral communication (lecture, 1987). [h] The shift was estimated, since the structure with H bridging the FeFe hinge is in equilibrium in solution with the one in which the endo hydrogen bridges a $BFe_w$ edge. Housecroft, C. E.; Shongwe, M. S.; Rheingold, A. L. *Organometallics* **1989**, *8*, 2651. Housecroft, C. E.; Rheingold, A. L. *Organometallics* **1987**, *6*, 1332. The boride radius is doubtful (there is no $Au^1Au^3$ bond). FeFe distances are not reported and are assumed from the related structures. [i] Harpp, K. S.; Housecroft, C. E.; Rheingold, A. L.; Shongwe, M. S. *J. Chem. Soc., Chem. Commun.* **1988**, 965. [j] Harpp, K. S.; Housecroft, C. E. *J. Organomet. Chem.* **1988**, *340*, 389. Housecroft, C. E. *Polyhedron* **1987**, *6*, 1935. [k] Hong, F.-E.; Coffy, T. J.; McCarthy, D. A.; Shore, S. G. *Inorg. Chem.* **1989**, *28*, 3284. [l] Khattar, R.; Puga, J.; Fehlner, T. P. *J. Am. Chem. Soc.* **1989**, *111*, 1877.

**Table II.** Oxygen Shifts for Semi-Interstitial and Capping Oxygens in Metal Clusters and Some Comparison Compounds

| compound | $\delta(^{17}O)$[a]/ppm | geometry[b] | r(O)/pm | ref |
|---|---|---|---|---|
| $[Fe_3Mn(CO)_{12}(\mu_4\text{-}O)]^-$ | 93 | butterfly, $Mn_w$ | 61.3 | *c* |
| $[Fe_3(CO)_9(\mu_3\text{-}O)]^{2-}$ | 107 | capping O | | *c* |
| $[Fe_2Ru_3(CO)_{14}(\mu_4\text{-}O)]^{2-}$ | 156 | sq pyramid, Ru(ap), capping O | | *d* |
| CO(g) | 350.2 | | | *e* |
| polyoxomolybdates | −30 to −50 | 6-coordinate O | | *f* |
| | 30–55 | 5-coordinate O | | |
| | 110–140 | 4-coordinate O | | |
| | 230–330 | 3-coordinate O | | |
| | 350–710 | 2-coordinate O | | |
| | 810–950 | terminal O | | |

[a] Relative to $H_2O(l)$. [b] (ap) means apical. [c] Schauer, C. K.; Shriver, D. F. *Angew. Chem., Int. Ed. Engl.* **1987**, *26*, 255. [d] Schauer, C. K.; Voss, E. J.; Sabat, M.; Shriver, D. F. *J. Am. Chem. Soc.* **1989**, *111*, 7662. [e] Wasylishen, R. E.; Mooibroek, S.; MacDonald, J. B. *J. Chem. Phys.* **1984**, *81*, 1057. [f] See e.g.: Klemperer, W. G. *Angew. Chem., Int. Ed. Engl.* **1978**, *17*, 246. Chauveau, F. *Bull. Soc. Chim. Fr.* **1986**, *2*, 199. Fedotov, M. A.; Kazanskii, L. P.; Spitsyn, V. I. *Dokl. Chem. (Engl. Transl.)* **1983**, *272*, 777. Maksimovskaya, R. I.; Fedotov, M. A. *J. Struct. Chem. (Engl. Transl.)* **1981**, *22*, 129. Kazanskii, L. P. *Coord. Chem.* **1977**, *3*, 240 [*Koord. Khim.* **1977**, *4*, 327].

The shifts of some simple molecules are shown in Figures 1–4 (which are lined up with $BH_4^-$, $CH_4$, $NH_4^+$, and $H_2O$ level) to illustrate the similar positions taken by corresponding (isoelectronic, isostructural) compounds. Such correspondences are normally found in charts with this scaling for elements with a close periodic relationship, such as neighbors in a row or group; thus correlations of boron and carbon shifts in analogous compounds are well-known,[14] as are similar correlations of carbon and nitrogen shifts.[15] For boron, carbon, nitrogen, and oxygen, high shielding is observed (all three factors in the paramagnetic term acting to reduce $|\sigma_p|$) in singly bonded compounds, such as boranes, alkanes, amines, ethers, or alcohols. The shielding decreases from saturated to linear groups, then to aromatics, and then to doubly bonded compounds, in which the paramagnetic circulation is mediated by relatively low-energy circulations of $\sigma \leftrightarrow \pi$ type. The nitrogen and oxygen ranges are extended (relative to the carbon range) in planar groups with low-energy $n \rightarrow \pi^*$ circulations: thus $O_3$ has very low oxygen shielding, $\delta(^{17}O)$ = 1032 ($O_t$) and 1598 ($O_c$),[16] all three factors in the paramagnetic term acting to increase $|\sigma_p|$ for the central oxygen ($O_c$).

Figure 1 and Table I show that the octahedrally coordinated borides $[Ru_6B(CO)_{17}]^-$ and $[Fe_4Rh_2B(CO)_{16}]^-$ exemplify the $\delta/r$ correlation as observed for the carbides and nitrides. Points representing gold-adduct cluster borides are shown in parentheses, the carbide–nitride study[10] having shown that considerable scatter is introduced into the correlation by irregularity in the cavity, whether produced by collapse of a larger cavity, asymmetric disposition of external ligands or capping groups, or the presence of disparate groups, as in Au–phosphine adducts of earlier transition metal clusters. Scatter arises also from differences in their geometries in solution (in which $\delta$(I) is measured) and the solid state (in which $r$(I) is measured).

The unusual shift pattern[17] that began to emerge with the first clusters observed to contain interstitial nitrogen, the rhodium and cobalt trigonal prisms,[18] is that whereas interstitial carbide is quite strongly deshielded, appearing below the normal range of shifts for organic compounds (Figure 2), the shielding of the corre-

(14) See e.g.: Nöth, H.; Wrackmeyer, B. *NMR Spectroscopy of Boron Compounds*; Springer-Verlag: Berlin, 1978. Kennedy, J. D. In ref 1, Chapter 8.

(15) Mason, J. In ref 1, Chapter 12; *Chem. Br.* **1983**, 654; *Chem. Rev.* **1981**, *81*, 205.

(16) See e.g.: McFarlane, W.; McFarlane, H. C. E. In ref 1, Chapter 14.

(17) Mason, J. In ref 1, p 357.

(18) Martinengo, S.; Ciani, G.; Sironi, A.; Heaton, B. T.; Mason, J. *J. Am. Chem. Soc.* **1979**, *101*, 7095.

**Table III.** Shielding Parameters (ppm), Interatomic Distances ($R_{MC}$/pm), and Radii ($r_C$/pm) for Interstitial Carbide in Metal Clusters

| cluster[a] | $\delta$ | $\sigma_{abs}$ | $R$(MC) | $\sigma_d^{AL}$ | $\sigma_p^{AL}$ | $r$(C) | ref |
|---|---|---|---|---|---|---|---|
| $[Rh_6(\mu_6\text{-}C)(CO)_{15}]^{2-}$, tp | 265 | −78 | 213.4 | 1456 | −1534 | 73.5 | *b* |
| $[Co_6(\mu_6\text{-}C)(CO)_{15}]^{2-}$, tp | 330 | −144 | 195 | 1048 | −1192 | 67.2 | *c* |
| $[Co_8(\mu_8\text{-}C)(CO)_{18}]^{2-}$, dist sa | 388 | −201 | 188 (av) | 1346 | −1548 | 73, 89 | *c* |
| $[Os_{10}(\mu_6\text{-}C)(CO)_{24}(\mu_4\text{-}H)]^-$, oct | 409 | −223 | 204 | 2367 | −2589 | 60.0 | *d* |
| $[Re_7(\mu_6\text{-}C)(CO)_{21}]^{3-}$, dist oct | 424 | −237 | 213 | 2252 | −2489 | 62.5 | *e* |
| $[Re_8(\mu_6\text{-}C)(CO)_{24}]^{2-}$, dist oct | 431 | −245 | 211.6 | 2265 | −2510 | 62.0 | *e* |
| $[Fe_3Ni_3(\mu_6\text{-}C)(CO)_{13}]^{2-}$, oct | 435 | −249 | (187) | 1081 | −1330 | (55.1) | *f* |
| $[Ru_6(\mu_6\text{-}C)(CO)_{16}]^{2-}$, oct | 459 | −272 | 204.5 | 1480 | −1752 | 61.3 | *g* |
| $[(\mu_2\text{-}H)Rh_6(\mu_6\text{-}C)(CO)_{13}]^-$, dist oct | 460 | −274 | 204.6 | 1480 | −1754 | 59.5 | *h* |
| $[RhFe_3(\mu_4\text{-}C)(CO)_{12}]^-$, bu | 461 | −275 | 192.7 (av) | 866 | −1141 | 59.6 (av) | *f* |
| $[(\mu_2\text{-}H)Fe_4(\mu_4\text{-}C)(CO)_{12}]^-$, bu | 464 | −278 | 189 | 784 | −1062 | 58.0 | *i* |
| $[Fe_4(\mu_4\text{-}C)(CO)_{13}]$, bu | 469 | −282 | 189.5 | 783 | −1065 | 58.4 | *j* |
| $[Rh_6(\mu_6\text{-}C)(CO)_{13}]^{2-}$, oct | 470 | −284 | 204.6 | 1507 | −1790 | 59.3 | *h* |
| $[CoFe_4(\mu_5\text{-}C)(CO)_{14}]^-$, sp | 477 | −290 | 187.8 (av) | 923 | −1213 | 57.6 (av) | *f* |
| $[Fe_4(\mu_4\text{-}C)(CO)_{12}]^{2-}$, bu | 478 | −292 | 188.3 | 786 | −1077 | 57.2 | *k* |
| $[Fe_6(\mu_6\text{-}C)(CO)_{16}]^{2-}$, oct | 485 | −298 | 188.6 | 1044 | −1342 | 55.5 | *k* |
| $[Fe_5(\mu_5\text{-}C)(CO)_{15}]$, sp | 486 | −300 | 190.4 (av) | 909 | −1208 | 57.9 (av) | *k* |

[a] tp = trigonal prism; sa = square antiprism; dist = distorted; oct = octahedron; bu = butterfly; sp = square pyramid. [b] Albano, V. G.; Chini, P.; Martinengo, S.; McCaffrey, D. J. A.; Strumolo, D.; Heaton, B. T. *J. Am. Chem. Soc.* **1974**, *96*, 8106. [c] Albano, V. G.; Chini, P.; Ciani, G.; Sansoni, M.; Strumolo, D.; Heaton, B. T.; Martinengo, S. *J. Am. Chem. Soc.* **1976**, *98*, 5027. $[Co_6(\mu_6\text{-}C)(CO)_{15}]^{2-}$ structure: Martinengo, S.; Strumolo, D.; Chini, P.; Albano, V. G.; Braga, D. *J. Chem. Soc., Dalton Trans.* **1985**, 35. [d] Constable, E. C.; Johnson, B. F. G.; Lewis, J.; Pain, G. N.; Taylor, M. J. *J. Chem. Soc., Chem. Commun.* **1982**, 754. [e] Ciani, G.; D'Alfonso, G.; Freni, M.; Romiti, P.; Sironi, A. *J. Chem. Soc., Chem. Commun.* **1982**, 339, 705. [f] Hriljac, J. A.; Swepston, P. N.; Shriver, D. F. *Organometallics* **1985**, *4*, 158. The core dimensions of $[Fe_3Ni_3(\mu_6\text{-}C)(CO)_{13}]^{2-}$, for which no structure was reported, were estimated by comparison with those of $[Co_6(\mu_6\text{-}C)(CO)_{13}]^{2-}$: Albano, V. G.; Braga, D.; Martinengo, S. *J. Chem. Soc., Dalton Trans.* **1986**, 981. [g] Bradley, J. S. *Adv. Organomet. Chem.* **1983**, *22*, 1. This reference corrects the $\delta(^{13}C)$ value given by: Bradley, J. S.; Ansell, G. B.; Hill, E. W. *J. Organomet. Chem.* **1980**, *184*, C33. [h] Bordoni, S.; Heaton, B. T.; Seregni, C.; Strona, L.; Hursthouse, M. B.; Thornton-Pett, M.; Martinengo, S. *J. Chem. Soc., Dalton Trans.* **1988**, 2103. This reference corrects the $\delta(^{13}C)$ value for $[Rh_6C(CO)_{13}]^{2-}$ given by: Heaton, B. T.; Strona, L.; Martinengo, S. *J. Organomet. Chem.* **1981**, *215*, 415. [i] Holt, E. M.; Whitmire, K. H.; Shriver, D. F. *J. Organomet. Chem.* **1981**, *213*, 125. [j] Bradley, J. S.; Ansell, G. B.; Leonowicz, M. E.; Hill, E. W. *J. Am. Chem. Soc.* **1981**, *103*, 4968. [k] Bradley, J. S. *Philos. Trans. R. Soc. London, A* **1982**, *308*, 103.

**Table IV.** Shielding Parameters (ppm), Interatomic Distances ($R$(MN)/pm), and Radii ($r$(N)/pm) for Interstitial Nitride in Metal Clusters

| cluster[a] | $\delta^b$ | $\sigma_{abs}$ | $R$(MN) | $\sigma_d^{AL}$ | $\sigma_p^{AL}$ | $r$(N) | ref |
|---|---|---|---|---|---|---|---|
| $[Rh_6(\mu_6\text{-}N)(CO)_{15}]^-$, tp | −273 | 137 | 213 | 1524 | −1387 | 73.9 | *c* |
| $[Co_6(\mu_6\text{-}N)(CO)_{15}]^-$, tp | −184 | 48 | 193.8 | 1118 | −1070 | 67.2 | *c* |
| $[Ru_{10}(\mu_6\text{-}N)(CO)_{24}]^-$, to | 34 | −170 | 205 | 1543 | −1713 | 61 | *d* |
| $[Ru_5(\mu_5\text{-}N)(CO)_{14}]^-$, sp | 85 | −221 | 205.6 | 1338 | −1559 | 64.0 | *e, f* |
| $[Ru_4(\mu_4\text{-}N)(CO)_{12}]^-$, bu | 139.5 | −275 | 199.5 | 1162 | −1437 | 61.2 | *e, g* |
| $[Fe_hRu_3(\mu_4\text{-}N)(CO)_{12}]^-$, bu | 140.5 | −276 | 195.9 (av) | 1091 | −1367 | 61 | *h* |
| $[Fe_wRu_3(\mu_4\text{-}N)(CO)_{12}]^-$, bu | 179.6 | −315 | 195.9 (av) | 1091 | −1406 | 59 | *h* |
| $[Ru_6(\mu_6\text{-}N)(CO)_{16}]^-$, oct | 180 | −316 | 205 | 1543 | −1859 | 61[h] | *e, f* |
| $[Fe_4(\mu_4\text{-}N)(CO)_{12}(\mu_2\text{-}H)]$, bu | 211 | −347 | 184.5 | 883 | −1209 | 54.3 | *e, i* |
| $[Fe_4(\mu_4\text{-}N)(CO)_{12}]^-$, bu | 239 | −374.5 | 183.5 | 865 | −1240 | 54.2 | *e, j* |

[a] tp = trigonal prism; to = tetracapped octahedron; oct = octahedron; bu = butterfly; sp = square pyramid. Subscripts h and w label hinge and wingtip metals. $\mu_2$-H bridges the MM hinge. [b] Relative to neat liquid nitromethane. [c] Martinengo, S.; Ciani, G.; Sironi, A.; Heaton, B. T.; Mason, J. *J. Am. Chem. Soc.* **1979**, *101*, 7095. [d] Bailey, P.; Johnson, B. F. G.; Lewis, J.; Wilkinson, D. Unpublished work. The cavity dimensions are taken from those of related structures. [e] Gladfelter, W. L. *Adv. Organomet. Chem.* **1985**, *24*, 41. [f] Blohm, M. L.; Gladfelter, W. L. *Organometallics* **1985**, *4*, 45. [g] Harris, S.; Blohm, M. L.; Gladfelter, W. L. *Inorg. Chem.* **1989**, *28*, 2290. [h] The radii are estimated (by comparison with other Fe and Ru butterfly structures) from the averaged values observed for the disordered structure: Fjare, D. E.; Gladfelter, W. L. *J. Am. Chem. Soc.* **1984**, *106*, 4799. [i] The cavity dimensions are taken from those of the isostructural carbide given by: Tachikawa, M.; Stein, J.; Muetterties, E. L.; Teller, R. G.; Beno, M. A.; Gebert, E.; Williams, J. M. *J. Am. Chem. Soc.* **1980**, *102*, 6648. [j] Blohm, M. L.; Fjare, D. E.; Gladfelter, W. L. *Inorg. Chem.* **1983**, *22*, 1004.

sponding (isostructural, isoelectronic) interstitial nitride lies within the organic range[15] (Figure 3). (There was an apparent anomaly in that the carbon shielding in octahedral clusters was first reported to be relatively high, but two early values for the carbon shieldings have now been corrected, as noted in the footnotes of Table III.) The higher shielding of the nitrides correlates with (de)compression,[10] since interstitial carbon is compressed beyond the normal covalent radius for tetrahedral carbon (77 pm), whereas in the nitride clusters (in Figure 3) the most highly shielded nitrogen, in the $Rh_6$ trigonal prism ($r$(N) ≈ 74) pm), is "expanded" rather than compressed relative to the covalent radius (70 pm) for tetrahedrally coordinated nitrogen; furthermore, compression in the other nitrides is much reduced compared to the corresponding carbides (the metal cores are somewhat contracted in the nitrides compared to the corresponding carbides[19]). In the carbides, highest shielding is observed for trigonal prisms of rhodium ($r$(C) ≈ 74 pm) and cobalt ($r$(C) ≈ 67 pm), and lowest shielding for iron clusters with small cavities, whether octahedral, square pyramidal, or butterfly ($r$(C) ≈ 57 pm). In the trigonal prisms, the deshielding with compression (that is, in the cobalt compared to the rhodium cluster) is greater for the carbides than the nitrides, but the deshielding for the octahedron-based clusters (including the square pyramid and the butterfly) relative to the trigonal prisms is greater for the nitrides. The trigonal prisms have nitride shifts comparable to those in amines, and the nitride shifts in the octahedral, square-pyramidal, and butterfly clusters are comparable to those in diazenes or azo compounds. Interestingly, the interstitial phosphides so far measured show relatively low phosphorus shielding.[20]

The interstitial borides (Figure 1) continue the carbide–nitride pattern, as they are strongly compressed, with $r_B$ ≈ 57–61 pm in the octahedral clusters, compared to the normal covalent radius for 4-coordination (80 pm), and show very low boron shielding, well below the range[14] observed for organoboron compounds and boranes.

(19) Gladfelter, W. L. *Adv. Organomet. Chem.* **1985**, *24*, 41 and references therein.

(20) Mason, J. Manuscript in preparation.

The (butterfly) interstitial oxide now measured[21] is somewhat compressed ($r$(O) = 61 pm) compared to the covalent radius of oxygen (66 pm), the cluster being formed by small transition metals ($Fe_3Mn$). Interestingly, the oxygen shielding is high in the organic range,[16] not far below that of water and ethers (Figure 1). The capping oxygen so far measured[21,22] shows relatively high shielding (Table II), as do capping boron, carbon, and nitrogen,[20] compression being relieved by the displacement outside the cluster; capping oxygen is a 4-electron donor,[23] whereas all 6 electrons are contributed in the butterfly.[21]

Among the comparison shifts given in Table II and Figure 4 are $\delta(^{17}O)$ ranges observed for polyoxomolybdates, following the observation[21] that the capping $\mu_3$-O and the butterfly $\mu_4$-O follow the sequence of increase in shielding with increase in coordination number as in polyoxometalates, although the lower shielding for the $\mu_4$-O capping $Fe_2Ru_2$ reverses the trend.[22] In oxometalates, the main paramagnetic circulation is of oxygen p($\pi$) electrons in M–O LUMOs. The oxygen shielding decreases with increase in the MO bond order and decreases across the row of the metal (as the LUMOs stabilize). Significantly, the oxygen shielding increases down the group of the metal and with increase in coordination by M.

In bimetallic butterfly nitrides, the interstitial shift is observed to depend on the nature of the wingtip rather than the hinge metals.[19,23] Butterfly clusters show a further shielding–compression correlation, involving the $M_wIM_w$ angle, where $M_w$ is a wingtip metal. The dihedral angle, though rather variable, is normally larger in the borides than the 109° angle of the arachno-octahedron (with loss of two vertices) but is greatly reduced in the carbides and nitrides, sometimes below 100°. Some compression is relieved by deviation from linearity of the $M_wIM_w$ bonds, and there is a pleasing correlation of this angle with the interstitial shift. The $Fe_wCFe_w$ angle decreases from 178° in $[Fe_4(\mu_4\text{-}C)(CO)_{12}]^{2-}$ to 175° in $[Fe_4(\mu_4\text{-}C)(CO)_{13}]$, 174° in $[(\mu_2\text{-}H)Fe_4(\mu_4\text{-}C)(CO)_{12}]^-$, and 173° in $[RhFe_3(\mu_4\text{-}C)(CO)_{12}]^-$, the carbon shielding increasing over a range of 17 ppm, as compression is relieved (and similarly for the nitrides).

Observations in butterfly chemistry that may be related to compression of the interstitial atom include the occupation of a hinge position by the heterometal M in $Fe_3M$ carbides, when M is Rh, Mn, W, or Cr,[23] $r$(M) being larger than $r$(Fe); cf. the wingtip position of Mn in the $Fe_3Mn$ butterfly oxide.[21] Isomeric $FeRu_3N$ butterfly clusters with iron at the wingtip or at the hinge coexist in equilibrium in solution, the isomer with wingtip Fe predominating, and the two species cocrystallize with disorder of the iron, of which 74% occupies a wingtip position.[24] Analysis of the equilibrium in solution (by $^{13}C$ NMR spectroscopy of the carbonyls at 25–68 °C) gave a rather small enthalpy difference between the two isomers, $\Delta H = -3.5 \pm 1$ kcal mol$^{-1}$, and a quite large entropy difference, $\Delta S = -13 \pm 2$ eu, for which an explanation was suggested in terms of ion pairing with the PPN cation. The difference in compression of the nitride in the two structures may be significant also.

**Periodicities in the Factors Determining the Interstitial Shielding.** The increase in shielding of the interstitial element across the row can be rationalized in terms of the paramagnetic (p–p) circulation, since this is absent ($\sigma_p = 0$) in a closed shell, and the anions ($B^{5-}$, $C^{4-}$, $N^{3-}$, $O^{2-}$) become more stable across the row. Charge on the interstitial is reduced by the covalent bonding to the metal, which potentiates the paramagnetic circulation. The low shielding of interstitial carbon has been taken as evidence for a positive atomic charge,[25] but Fenske–Hall (FHMO) calculations show a moderate negative charge, −0.60e for $[Fe_4C(CO)_{12}]^{2-}$,[26] about −0.65e for $[HFe_4C(CO)_{12}]^-$ and $[Fe_4C(CO)_{13}]$,[27] and −0.8e for $[Ru_6C(CO)_{17}]$.[28] Extended Hückel (EHMO) calculations show the negative charge to increase with the size of the cavity,[29] as expected. There is NMR evidence for negative charge on the interstitial: thus the $^{13}C$ shielding of carbonyl ligands increases (by up to 10 ppm) in the presence of interstitial carbon, and carbonyl carbon is known to be shielded by electron-demanding coligands or by decrease in negative charge on the complex.

Covalent interaction with the metal is relatively strong for borides and carbides[30] and decreases across the row with increasing mismatch of the M–I energies. FHMO calculations[31] on the $[Fe_4X(CO)_{12}]^{q-}$ butterflies (X = C, N, O) show the p(X)–$Fe_w$ (d,s,p) overlap decreasing, C > N > O (so that the O–$Fe_w$ interaction may not be strong enough to maintain the cluster geometry). The splittings ($\Delta E$) of the p(X) orbital increase in this sequence, and this also acts to increase the interstitial shielding.

As the figures and tables show, the interstitial shielding increases strongly down the group of the metal for a given cluster symmetry. While correlating with relief from compression, this trend accords with stronger M–I overlap and smaller excitation energies when M is a metal of the first transition series, although changes from the second to the third series should be small on this basis. Increase in shielding down the group of the metal is observed also for ligating atoms in metal complexes, the increments being larger the closer the ligating atom is to the metal, as in nitrides triply bonded to the metal.[32] In back-bonding ligands (such as CO or $N_2$), the shielding of the ligating atom increases also from left to right across the transition series,[12] as observed to some degree in the clusters.

**Effects of Cluster Symmetry.** Figures 2 and 3 suggest that there are different lines of correlation with the nature of the metal for the different symmetries. The higher shielding in the trigonal prisms than in the octahedron-based clusters correlates with poorer M–I overlap and larger orbital splittings in the trigonal prisms.

A striking feature of Figure 2 is the similarity of the chemical shifts for octahedral, square-pyramidal, and butterfly clusters of iron; the spread is somewhat greater for the corresponding ruthenium nitrides as shown in Figure 3. Although the patterns of cluster energy levels are similar for these octahedron-based symmetries, compensating factors are likely to be at work. Conceivably, the contribution of lower energy circulations of weakly bonding electrons on the interstitial atom in the butterfly and square-pyramidal clusters might compensate for the smaller number of M–C interactions; indeed, it is curious that the $\delta$(I)/$r$(I) correlations include these clusters, in which the interstitital atom is somewhat exposed. These heteroatoms, however, resemble the ones that are totally enclosed in contributing all their valence electrons to the cluster electron count, in $\pi$- and $\sigma$-bonding;[19,33,34] quasi-lone-pair electrons are involved in $\pi$-bonding to the metal. Although interstitial carbide or nitride in square-pyramidal clusters has a somewhat larger atomic radius than in butterfly or octahedral clusters of the same metal and lies slightly below the basal plane, it is still within the van der Waals radius of the basal metals,[35] and is unreactive, as in octahedral clusters. Interstitial carbide or nitride in butterfly clusters is more reactive but not highly so: the first site of protonation is on the hinge in homometallic clusters, and reactivity is related to opening up of the

(21) Schauer, C. K.; Shriver, D. F. *Angew. Chem., Int. Ed. Engl.* **1987**, *26*, 255.
(22) Schauer, C. K.; Voss, E. J.; Sabat, M.; Shriver, D. F. *J. Am. Chem. Soc.* **1989**, *111*, 7662.
(23) Hriljac, J. A.; Swepston, P. N.; Shriver, D. F. *Organometallics* **1985**, *4*, 158.
(24) Fjare, D. E; Gladfelter, W. L. *J. Am. Chem. Soc.* **1984**, *106*, 4799.
(25) Albano, V. G.; Chini, P.; Martinengo, S.; McCaffrey, D. J. A.; Strumolo, D.; Heaton, B. T. *J. Am. Chem. Soc.* **1974**, *96*, 8106.
(26) Harris, S.; Bradley, J. S. *Organometallics* **1984**, *3*, 1086.
(27) Benson, C. G.; Long, G. J.; Bradley, J. S.; Kolis, J. W.; Shriver, D. F. *J. Am. Chem. Soc.* **1986**, *108*, 1898.
(28) Wales, D. J.; Stone, A. J. *Inorg. Chem.* **1989**, *28*, 3120.
(29) Halet, J.-F.; Evans, D. G.; Mingos, D. M. P. *J. Am. Chem. Soc.* **1988**, *110*, 87.
(30) Wijeyesekera, S. D.; Hoffmann, R. *Organometallics* **1984**, *3*, 949.
(31) Harris, S.; Blohm, M. L.; Gladfelter, W. L. *Inorg. Chem.* **1989**, *28*, 2290.
(32) Hughes, M.; Mason, J.; Richards, R. L. Unpublished work.
(33) Bradley, J. S. *Adv. Organomet. Chem.* **1983**, *22*, 1 and references therein.
(34) Wijeyesekera, S. D.; Hoffmann, R.; Wilker, C. N. *Organometallics* **1984**, *3*, 962.
(35) Henrick, K.; McPartlin, M.; Morris, J. *Angew. Chem., Int. Ed. Engl.* **1986**, *25*, 853.
(36) Halet, J.-F.; Saillard, J.-Y.; Lissillour, R.; McGlinchey, M. J.; Jaouen, G. *Organometallics* **1986**, *5*, 139.

angle, or flapping[33] (the carbide becoming more reactive with deviations from linearity of $M_wCM_w$). Oxide is less stable to sustain such $\pi$-bonding in square-pyramidal clusters; the 2p electrons are low-lying, this favoring their localization as lone pairs, and the heteroatom moves to a capping position;[35] cf. also the small $M_wOM_w$ angle in the butterfly, 168°.[21]

**Protonation Shifts.** For cluster "semi-interstitials", there is a measure of the deshielding attributable to low-energy circulations in $\pi$ or $\sigma$ LUMOs of quasi-lone-pair electrons, in the increase in shielding on protonation, that is, when a high lying electron pair is stabilized ($\Delta E$ is increased) by bonding to hydrogen.[37] The deshielding in the unprotonated form is analogous to the deshielding by n → $\pi^*$ circulations that plays a large part in nitrogen-shielding patterns, a benchmark value being the increase in nitrogen shielding by 100 ppm from pyridine to the pyridinium ion.[15] Protonation of $[FeRu_3N(CO)_{10}\{P(OMe)_3\}_2]^-$ both at the hinge and at nitrogen to give the $\mu_4$-NH compound greatly increases the nitrogen shielding, by 231 ppm.[38] Protonation of the hinge-protonated carbide $[HFe_4C(CO)_{12}]^{2-}$ to give the $\mu_4,\eta^2$-CH compound increases the carbon shielding by a correspondingly large amount, 129 ppm.[39] The increase with hinge protonation of $[Fe_4C(CO)_{12}]^{2-}$ is much smaller, 14 ppm; cf. 28 ppm for the isoelectronic and isostructural nitride $[Fe_4N(CO)_{12}]^-$, this being another example of the 2:1 ratio of nitrogen and carbon shifts. (The radius of the interstitial cavity is increased by a small amount, 0.1 ppm for the nitride and 0.8 pm for the more compressed carbide.) It is interesting that the protonation of a metal-based HOMO affects the carbon shift to this extent. Protonation of the $[Rh_6C(CO)_{13}]^{2-}$ octahedron increases the carbon shielding by 10 ppm (barely increasing the carbon radius).

A simple example of a protonation shift is not yet available for a cluster boride, but there is a sizable increase in shielding (again, with "scaling" by the radial factor) of 32 ppm from $[HRu_4(\mu_4\text{-}BH)(CO)_{12}]^-$ to $[HRu_4(\mu_4\text{-}BH_2)(CO)_{12}]$,[40] and similarly for the $Fe_4$ analogues (34 ppm), as shown in Table I. The effect of addition of $AuPR_3$ to the interstital is smaller (as might be expected with formation of a weaker bond).

The large protonation shifts of butterfly interstitials reflect the large contribution to the (de)shielding of the interstitial by low-energy circulations of quasi-lone-pair electrons. A contribution of this type is likely in square-pyramidal clusters also (even though protonation may not be achievable).

**The Diamagnetic Contribution.** A shielding contribution that is commonly neglected is that arising from diamagnetic circulations on neighboring atoms, but this has been found to be important when the neighbors are heavy atoms. In Ramsey shielding theory, the diamagnetic and paramagnetic terms are summed over the whole molecule and each increases with increase in molecular size.[11,12] It is customary to assume the cancellation of "distant" diamagnetic and paramagnetic contributions to the shielding of a nucleus (A), since $\sigma_d$ contributions are $(r^{-1})$-dependent and $\sigma_p$ contributions become so (through the angular momentum term $\langle 0|L^2|0\rangle$, the moment of an electron depending on the distance). In organic molecules, the term "distant" is commonly taken to include nearest neighbors (and variations in $\sigma_d$ may then be neglected, as they are usually small in comparison with variations in $\sigma_p$). This "atom-in-a-molecule" approach has been shown to be inadequate[11] when the immediate neighbors are heavy atoms, particularly when changes in $|\sigma_p|$ are relatively small, as for light atoms.

A less drastic approximation is an "atom-plus-ligand (L)" or, in this case, atom-plus-neighbor (N) approach in which $\sigma_d^{AN}$ and $\sigma_p^{AN}$ terms sum over orbitals on the immediate neighbors (N) as well as those on A and longer range contributions can be neglected with more confidence. Thus a two-center (M–H) approach was used by Buckingham and Stephens[41] to show that high shielding of hydrides in transition-metal complexes arises from d–d circulations on the metal. An "atom-plus-ligands" model was used to explain the sagging or U-shaped plot of $\delta(^{13}C)$ against $n$ in $CX_nY_{4-n}$ compounds in terms of partial cancellation of (more regular) increments in $\sigma_d^{AL}$ and $\sigma_p^{AL}$,[11] and recent ab initio calculations of tin shielding in $SnX_nY_{4-n}$ compounds have shown the importance of increments in $\sigma_d$ as well as as $\sigma_p$ with change in the number of chloro ligands.[42] As an exception to the linearity of the plots of $\sigma_p^{AL}$ against $n$,[11] there was a shortfall in the paramagnetic contribution for $CI_4$ (and to a lesser extent, $CBr_4$), which was subsequently explained in terms of relativistic effects of the very heavy atoms.[12]

It has not been possible to calculate paramagnetic terms for molecules of the complexity of these clusters because of lack of knowledge of the orbital energies, but $\sigma_p^{AN}$ terms can be obtained by difference, by use of $\sigma = \sigma_d^{AN} + \sigma_p^{AN}$. The shielding $\sigma$ is readily obtained for nuclei for which an absolute scale (relative to the bare nucleus) has been established. For carbon, $\sigma = 186.4 - \delta$,[43] and for nitrogen, $\sigma = -135.8 - \delta$.[44] Diamagnetic terms can be reliably calculated by the Flygare method, which gives[45]

$$\sigma_d^{AL} = \sigma_d(\text{free atom}) + (\mu_0/4\pi)(e^2/2m)\sum_N Z_N/R_N$$

where $\sigma_d$(free atom) is 267.2 ppm for carbon and 333.2 ppm for nitrogen.[46] The sum is taken over immediate ligands $N$ (that is, the metals of the cluster, excluding any capping metals), where $Z_N$ is the atomic number and $R_N$ the M–I distance.

$\sigma_p^{AN}$ is then the deshielding of the interstitial nucleus arising from paramagnetic currents on the interstitial and the (immediate) cluster metals. As shown in Tables III and IV, there are varying degrees of cancellation by the $\sigma_d^{AN}$ terms, depending on the nature of the cluster. Particularly for changes in cluster nuclearity, and from the first to the second and the third transition series, the increments are large, and differences between them are comparable with changes in the local shielding terms (arising from circulations of the atom's "own" electrons).

The values for the $Fe_4$, $Fe_5$, and $Fe_6$ carbides show that the small effects of increase in nuclearity on the observed shifts are the resultant of similar and compensating diamagnetic and paramagnetic increments. In the $Ru_4$, $Ru_5$, and $Ru_6$ nitrides, there is a smaller increase in the paramagnetic component ($|\sigma_p^{AN}|$) from the butterfly to the square prism (in which the cavity radius is 64 pm compared with 61 pm in the butterfly), then a larger increase to the (compressed) octahedron (61 pm), and the resultant shielding changes are irregular. The small increase in shielding across the row of the metal from the $Fe_6$ to the $(FeNi)_3$ octahedral carbides, and the $Fe_4$ to $Ru_4$ butterfly nitrides, arises from an increase in the diamagnetic component outweighing the increase in paramagnetic component. The $Ru_6$ and $Rh_6$ octahedral carbides, however, show a decrease in shielding across the row, following a small increase in $|\sigma_p^{AN}|$ to the (slightly more compressed) $Rh_6$ octahedron.

Down the group of the metal, however, the diamagnetic contribution outweighs the paramagnetic contribution in each case. Interestingly, in the tetracapped $Ru_{10}N$ octahedron and perhaps also in the $Os_{10}C$ analogue there is increased shielding of the interstitial compared to simple octahedra.

## Conclusion

It is curious that interstitial shieldings correlate as well as they do with compression in the cavity, given the multiplicity of the

(37) Grieves, R. A.; Mason, J. *Polyhedron* **1986**, *5*, 415.
(38) Blohm, M. L.; Fjare, D. E.; Gladfelter, W. L. *J. Am. Chem. Soc.* **1986**, *108*, 2301.
(39) Tachikawa, M.; Muetterties, E. L. *J. Am. Chem. Soc.* **1980**, *102*, 4541.
(40) Chipperfield, A. K.; Housecroft, C. E.; Rheingold, A. L. *Organometallics* **1990**, *9*, 681.
(41) Buckingham, A. D.; Stephens, P. J. *J. Chem. Soc.* **1964**, 2747, 4583.
(42) Nakatsuji, H.; Inoue, T.; Nakao, T. *Chem. Phys. Lett.* **1990**, *167*, 111.
(43) Jameson, A. K.; Jameson, C. J. *Chem. Phys. Lett.* **1987**, *134*, 461.
(44) Jameson, C. J.; Jameson, A. K.; Opposungguu, E.; Wille, S.; Burrell, P. M.; Mason, J. *J. Chem. Phys.* **1981**, *74*, 81.
(45) Flygare, W. H.; Goodisman, J. *J. Chem. Phys.* **1968**, *49*, 3122. Gierke, T. D.; Tigelaar, H. L.; Flygare, W. H. *J. Am. Chem. Soc.* **1972**, *94*, 330. Gierke, T. D.; Flygare, W. H. *J. Am. Chem. Soc.* **1972**, *94*, 7277.
(46) Lederer, C. M.; Shirley, V. S. *Tables of Isotopes*, 7th ed.; Wiley: New York, 1978; Appendix VII.

factors involved. The large increases in shielding on direct protonation of butterfly interstitials show that an important component of their low shielding is due to low-energy circulations of quasi-lone-pair electrons (weakly bonding to the metal), and a contribution of this type is likely in square-pyramidal clusters also.

It is likely that the significant factors in the patterns of interstitial shieldings include not only the ones that determine the local paramagnetic circulation but also those determining the diamagnetic and paramagnetic circulations on the cluster metal, which are not negligible within the cluster. The sizable increase in shielding down the group of the metal (for a given symmetry) shows the importance of the diamagnetic contribution most clearly. This parallels the increase in shielding with the coordination number of oxygen in polyoxometalates (cf. Table II and Figure 4) and the increases in shielding observed for non-metals and metals with heavy substituents, such as the heavier halogens. It is likely that relativistic contributions to the shielding of the interstitial will be important with the heaviest metals, Au in particular, and that the effects of heavy neighbors will be particularly marked in the shielding of the lightest interstitial, hydride.[20]

**Acknowledgment.** I am grateful to the Leverhulme Trust for a fellowship.

# Effects of Positions of Donor and Acceptor Type Substituents on Ground- and Excited-State Charge Transfer: Electrochromism of Some Benzene Derivatives

**Hemant K. Sinha and Keith Yates***

*Contribution from the Department of Chemistry, Lash Miller Chemical Laboratories, University of Toronto, Toronto, Ontario, Canada M5S 1A1.* *Received October 22, 1990. Revised Manuscript Received April 15, 1991*

**Abstract:** 4-$NO_2$, 3-$NO_2$, and 3,5-di-$NO_2$ substituents as acceptors (A) relative to 1-$NH_2$, 1-OMe, and 1-C≡CH as donors (D) on the benzene ring have been examined in order to understand the relation between position of D and A moieties relative to each other and the charge distribution in the ground and excited states. Ground-state dipole moments ($\mu_g$) [obtained from dielectric measurements] in each case follow the order 4-$NO_2$ > 3,5-di-$NO_2$ > 3-$NO_2$. On the other hand, the excited-state dipole moments ($\mu_e$) and the change in dipole moment ($\Delta\mu$) [obtained from electrooptic measurements] show a different trend, i.e., 4-$NO_2$ > 3-$NO_2$ > 3,5-di-$NO_2$. In the excited state the charge migration from the donor site to the acceptor site in the meta isomer has been found to be comparable to that in the para isomer, and this supports the unusual meta effect found in various photochemical reactions. The observed changes have been interpreted with simple molecular orbital calculations, and a regular trend has been found in each case studied.

## Introduction

Intramolecular charge transfer (ICT) in organic molecules containing donor (D) and acceptor (A) groups has relevance to many aspects of physics and chemistry. For example, organic materials having strong charge-transfer characteristics are attractive for applications in nonlinear optics, such as frequency doubling of semiconductor lasers, electrooptic modulation of light, etc.[1,2] Charge transfer in the excited state can bring about very interesting chemical phenomena, such as twisting of the molecular skeleton,[3] intermolecular interactions,[4] unusual chemical reactivity, etc.[5] To understand such physical and chemical phenomena of excited states, it is essential to have a clear picture of the electrical properties of the molecule in its ground and electronically excited state. Experimentally, one step in this direction would be to examine how variations in the position of the same substituents effect the resultant charge distribution in both the ground and excited states, which has been attempted in this paper.

The most simple systems for which ICT has been well-recognized in the ground state are substituted benzenes containing donor and acceptor moieties.[6] The effect of the relative position of D and A type substituents on the electronic spectral characteristics have been elegantly discussed by McGlynn et al.[6] However, similar reports describing excited-state charge-transfer properties are scarce in the literature. In most reported experiments, the electronic spectral shift method (more commonly known as the solvatochromic method) has been used to determine the excited-state dipole moment, which reflects the charge-transfer character in the excited state.[7] This method has been considered to be a highly approximate procedure, particularly when the chromophores are strongly interacting in nature (termed specific interaction), due to the assumptions in the derivation and practical application of the formulas required for the calculations.

On the other hand, electrochromism permits the determination of dipole moment and polarizability of a nonequilibrium (Frank–Condon) state with relatively high precision, although even

(1) *Nonlinear Optical Properties of Organic Molecules and Crystals*; Chemla, D. S., Zyss, J. Eds.; Academic Press: New York, 1987; Vol. 1 and 2.

(2) *Nonlinear Optical Properties of Organic and Polymer Materials*; Williums, D. J. Ed.; Americal Chemical Society: Washington, DC, 1983; ACS Symposium Series 233.

(3) Rettig, W. *Angew. Chem., Int. Ed. Engl.* **1986**, *25*, 971. Lippert, E.; Rettig, W.; Bonacic-Koutecky, V.; Heisel, F.; Miehe, J. A. Photophysics of Internal Twisting. In *Advances in Chemical Physics*; Prigogine, I., Rice, S. A., Eds.; Wiley: New York, 1987; p 1.

(4) Davidson, R. S. The Chemistry of Excited State Complex: A Survey of Reactions. In *Advances in Physical Organic Chemistry*, *19*; Gold, V., Bethell, D., Eds.; Academic Press: New York, 1983; p 1.

(5) (a) Salem, L. *Acc. Chem. Res.* **1979**, *12*, 1979. (b) Zimmerman, H. E.; Sandel, V. R. *J. Am. Chem. Soc.* **1963**, *85*, 915. (c) Turro, N. J. In *Modern Molecular Photochemistry*; Benzamin/Cummings: U.S.A., 1985.

(6) (a) Carsey, T. P.; Findley, G. L.; McGlynn, S. P. *J. Am. Chem. Soc.* **1979**, *101*, 4502. (b) Findley, G. L.; Carsey, T. P.; McGlynn, S. P. *J. Am. Chem. Soc.* **1979**, *101*, 4511. (c) Rollison, A. M.; Drickamer, H. G. *J. Chem. Phys.* **1980**, *73*, 5981.

(7) (a) Lippert, E. *Angew. Chem.* **1961**, *73*, 695. (b) Mataga, N.; Kaifu, Y. and Kaizumi, M. *Bull. Chem. Soc. Jpn.* **1956**, *29*, 465. (c) Bakhshiev, N. G.; Knyazhanskii, M. I.; Minkin, V. I.; Osipov, O. A.; Saidov, G. V. *Russ. Chem. Rev.* **1969**, *38*, 740.

0002-7863/91/1513-6062$02.50/0 